Analysis of a Flat Annular Crack under Shear Loading

Hyeon Gyu Beom* and Youn Young Earmme*

(Received July 14, 1992)

An annular crack in an infinite isotropic elastic solid under shear loading is analyzed. General solution to the Navier's equilibrium equation is expressed in terms of three harmonic functions. Employing the Hankel transform the harmonic functions are represented by the solution of a pair of triple integral equations. The triple integral equations are reduced to a pair of mixed Volterra-Fredholm integral equations, which are numerically solved. The stress intensity factors of the annular crack under various shear loadings such as uniform radial shear, linearly varying radial shear, uniform shear and linearly varying shear are calculated as the Poisson's ratio ν and a/b (a; inner radius, b; outer radius) vary.

Key Words: Annular Crack, Hankel Transform, Triple Integral Equation, Mixed Volterra-Fredholm Integral Equation, Stress Intensity Factor, Shear Loading

1. Introduction

Studies on three-dimensional crack have been widely performed since the work by Sneddon(1946) for a penny-shaped crack. The results of the analysis of three-dimensional crack by many researchers are well documented recently in Panasyuk et al.(1981). Especially the problem of the annular crack has been an interesting subject due to its potential application to a frequently encountered banana-shaped crack (Moss and Kobayashi, 1971) or a three-dimensional crack blocked inside by a circular-shaped second phase particle without which the crack would have been penny-shaped. Smetanin(1968) used an asymptotic method to solve the problem of a flat annular crack subjected to uniaxial tension. Subsequently the analysis of the annular crack has been carried out by Moss and Kobayashi(1971), Choi and Shield(1982), Selvadurai and Singh (1985) and Danyluk and Singh(1986).

These works, however, are concerned with the annular crack under uniform pressure or torsion because of simpler mathematics involved: For the annular crack under uniform pressure or torsion, it is necessary to determine mathematically a single harmonic function. On the other hand, for the annular crack subjected to remote uniform shear (which is typical in application sense), the problem has not been solved yet since this requires a determination of two harmonic functions, making the task quite complicated.

It is the purpose of this study to investigate the problem of the annular crack in an infinite isotropic elastic solid under shear loading. Thus the crack front is in general under combined mode II and mode III loading. General solution to the Navier's equilibrium equation is expressed in terms of three harmonic functions. Employing the Hankel transform the harmonic functions are represented by a pair of triple integral equations. In cotrast to the previous works mentioned above, where a single harmonic function is determined, we here have to determine essentially two harmonic functions. Guided by a method for solving

* Department of Mechanical Engineering, Korea Advanced Institute of Science and Technology, 373-1 Kusong-Dong, Yusung-Gu, Taejon, 305-701, Korea

a triple integral equation proposed by Cooke(1963), we reduce a pair of the triple integral equations to a pair of mixed Volterra-Fredholm intergral equations, which are numerically solved by using the Simpson quadrature rule. The stress intensity factors of the annular crack under various shear loadings such as uniform radial shear, linearly varying radial shear, uniform shear and linearly varying shear are calculated as the Poisson's ratio ν and a/b (a; inner radius, b; outer radius) vary.

2. Formulation of the Problem

Suppose an annular crack is embedded in an infinite elastic solid, as shown in Fig. 1. The annular crack with the inner radius a and outer radius b lies in the plane $z=0$. Equal and opposite shear tractions are applied on the crack surface. The displacements $\boldsymbol{u}$ satisfy the Navier's equation of equilibrium:

$$\nabla^2\boldsymbol{u}+\frac{1}{1-2\nu}\nabla e=0,\quad e=\nabla\cdot\boldsymbol{u}, \tag{1}$$

where ν is the Possion's ratio and e denotes the dilatation. Introducing cylindrical coordinates (r,θ,z), a general solution of (1) is expressed in terms of three harmonic functions as

$$2\mu u_r=z\frac{\partial\phi}{\partial r}+\frac{\partial\chi}{\partial r}+\frac{1}{r}\frac{\partial\Psi}{\partial\theta},$$

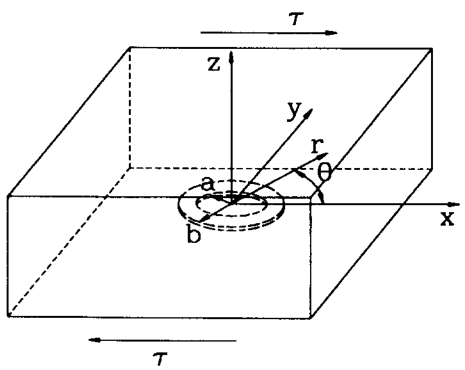

Fig. 1 An annular crack with inner radius a and outer radius b

$$2\mu u_\theta=\frac{z}{r}\frac{\partial\phi}{\partial\theta}+\frac{1}{r}\frac{\partial\chi}{\partial\theta}-\frac{\partial\Psi}{\partial r},$$

$$2\mu u_z=z\frac{\partial\phi}{\partial z}-(3-4\nu)\phi+\frac{\partial\chi}{\partial z}, \tag{2}$$

where μ is the shear modulus and ϕ, χ and Ψ are harmonic functions (See Appendix A). The corresponding stress components are given by

$$\sigma_r=z\frac{\partial^2\phi}{\partial r^2}-2\nu\frac{\partial\phi}{\partial z}+\frac{\partial^2\chi}{\partial r^2}+\frac{1}{r}\frac{\partial^2\Psi}{\partial r\partial\theta}-\frac{1}{r^2}\frac{\partial\Psi}{\partial\theta},$$

$$\sigma_\theta=-z\frac{\partial^2\phi}{\partial z^2}-z\frac{\partial^2\phi}{\partial r^2}-2\nu\frac{\partial\phi}{\partial z}-\frac{\partial^2\chi}{\partial r^2}-\frac{\partial^2\chi}{\partial z^2}-\frac{1}{r}\frac{\partial^2\Psi}{\partial r\partial\theta}+\frac{1}{r^2}\frac{\partial\Psi}{\partial\theta},$$

$$\sigma_z=z\frac{\partial^2\phi}{\partial z^2}-2(1-\nu)\frac{\partial\phi}{\partial z}+\frac{\partial^2\chi}{\partial z^2},$$

$$\tau_{r\theta}=\frac{z}{r}\frac{\partial^2\phi}{\partial r\partial\theta}-\frac{z}{r^2}\frac{\partial\phi}{\partial\theta}+\frac{1}{r}\frac{\partial^2\chi}{\partial r\partial\theta}-\frac{1}{r^2}\frac{\partial\chi}{\partial\theta}+\frac{1}{2r}\frac{\partial\Psi}{\partial r}-\frac{1}{2}\frac{\partial^2\Psi}{\partial r^2}+\frac{1}{2r^2}\frac{\partial^2\Psi}{\partial\theta^2},$$

$$\tau_{rz}=z\frac{\partial^2\phi}{\partial r\partial z}-(1-2\nu)\frac{\partial\phi}{\partial r}+\frac{\partial^2\chi}{\partial r\partial z}+\frac{1}{2r}\frac{\partial^2\Psi}{\partial\theta\partial z},$$

$$\tau_{\theta z}=\frac{z}{r}\frac{\partial^2\theta}{\partial\phi\partial z}-\frac{(1-2\nu)}{r}\frac{\partial\phi}{\partial\theta}+\frac{1}{r}\frac{\partial^2\chi}{\partial\theta\partial z}-\frac{1}{2}\frac{\partial^2\Psi}{\partial r\partial z}. \tag{3}$$

Arbitray loads applied to the crack surface can be expressed as a sum of symmetric and skew-symmetric parts. In this study, it is analyzed only the case in which the crack is sujected to a skew-symmetric loading. Due to the symmetry of the problem about the plane $z=0$, it is required that u_r and u_θ be odd functions fo z, while u_z is even in z. Therefore, we can restrict our attention to the analysis of a single half-space region $(z\geq 0)$ of the infinite space. The boundary conditions on the crack surface and along the plane of symmetry to be satisfied are:

$$\sigma_z(r,\theta,0)=0,\quad r\geq 0;\ 0\leq\theta<2\pi,$$

$$\tau_{zr}(r,\theta,0)=q_c(r,\theta),$$

$$a<r<b;\ 0\leq\theta<2\pi,$$

$$\tau_{z\theta}(r,\ \theta,\ 0)=q_s(r,\ \theta),$$
$$a<r<b;\ 0\leq\theta<2\pi,$$
$$u_r(r,\ \theta,\ 0)=u_\theta(r,\ \theta,\ 0)=0,$$
$$0\leq r<a,\ r>b;\ 0\leq\theta<2\pi, \quad (4)$$

where $q_c(r,\ \theta)$ and $q_s(r,\ \theta)$ are the given functions. In addition, the displacements and stresses approach zero as $\sqrt{r^2+z^2}\to\infty$. The specified functions $q_c(r,\ \theta)$ and $q_s(r,\ \theta)$ are expanded into cosine and sine Fourier series, respectively:

$$q_c(r,\ \theta)=\sum_{n=0}^{\infty}a_n(r)\cos n\theta,$$
$$q_s(r,\ \theta)=\sum_{n=0}^{\infty}b_n(r)\sin n\theta. \quad (5)$$

For simplicity of presentation, we assume here that $q_c(r,\ \theta)$ and $q_s(r,\ \theta)$ are even and odd functions of θ, however, this method can be easily modified to account for arbitrary $q_c(r,\ \theta)$ and $q_s(r,\ \theta)$.

In the region $z\geq 0$, the appropriate forms of the three harmonic functions ϕ, Ψ and χ are obtained from the Fourier-Hankel relations as (Kassir and Sih, 1975)

$$\phi(r,\ \theta,\ z)=\sum_{n=0}^{\infty}\cos n\theta\int_0^\infty\frac{A_n(s)}{s}\exp(-sz)J_n(rs)\,ds,$$
$$\Psi(r,\ \theta,\ z)=\sum_{n=1}^{\infty}\sin n\theta\int_0^\infty\frac{B_n(s)}{s}\exp(-sz)J_n(rs)\,ds,$$
$$\chi(r,\ \theta,\ z)=\sum_{n=0}^{\infty}\cos n\theta\int_0^\infty\frac{C_n(s)}{s}\exp(-sz)J_n(rs)\,ds, \quad (6)$$

where J_n denotes the Bessel function of order n and A_n, B_n and C_n are to be determined so as to satisfy the boundary conditions. In passing, it is worth mentioning that when the evenness and oddness in θ for the shear loads in (5) are interchanged, the $\cos n\theta$ and $\sin n\theta$ in (6) are also interachanged.

Since σ_z vanishes on $z=0$ (boundary condition (4)),

$$2(1-\nu)A_n(s)+sC_n(s)=0, \quad (7)$$

and the other boundary conditions (4) lead to a pair of simultaneous triple integral equations:

$$\int_0^\infty s\left[\frac{-1}{1-\nu}D_n(s)+E_n(s)\right]J_{n-1}(rs)\,ds$$
$$=\frac{1}{2}[a_n(r)-b_n(r)],\ a<r<b,$$
$$\int_0^\infty s\left[\frac{1}{1-\nu}D_n(s)+E_n(s)\right]J_{n+1}(rs)\,ds$$
$$=\frac{1}{2}[a_n(r)+b_n(r)],\ a<r<b, \quad (8a)$$
$$\int_0^\infty[-D_n(s)+E_n(s)]J_{n-1}(rs)\,ds=0,$$
$$0\leq r<a,\ r>b,$$
$$\int_0^\infty[D_n(s)+E_n(s)]J_{n+1}(rs)\,ds=0,$$
$$0\leq r<a,\ r>b, \quad (8b)$$

where

$$D_n(s)=-\frac{1-\nu}{2s}A_n(s),$$
$$E_n(s)=-\frac{1}{4}B_n(s), \quad (8c)$$

and $n=0,\ 1,\ 2,\ 3,\ \cdots$. In obtaining (8a) and (8b), the recurrence relations of the Bessel function

$$\frac{d}{dr}J_n(rs)=sJ_{n-1}(rs)-\frac{n}{r}J_n(rs),$$
$$J_n(rs)=\frac{rs}{2n}[J_{n-1}(rs)+J_{n+1}(rs)], \quad (9)$$

and (7) have been used. For the case of the Poisson's ratio $\nu=0$, it can be shown that (8a) and (8b) are reduced to two decoupled triple integral equations, as discussed by Cooke(1963). Also, it can be verified that for $n=0$ (radial shear), (8a) and (8b) are reduced to a triple integral equation.

3. Solution of Simultaneous Triple Integral Equations

Adopting a method which is in fact an extension of the technique proposed by Cooke(1963), it can be shown that a pair of the simultaneous triple integral Eqs. (8a) and (8b) can be reduced to a pair of the mixed Volterra-Fredholm integral equations. The solution procedure is lengthy and tedious, which is briefly described as follows. Details required for the solution are presented in Appendix B. Let

$$\int_0^\infty s\left[\frac{-1}{1-\nu}D_n(s)+E_n(s)\right]J_{n-1}(rs)\,ds = \begin{cases} f_1(r), & 0\le r<a,\\ f_2(r), & a<r<b,\\ f_3(r), & r>b,\end{cases}$$

$$\int_0^\infty s\left[\frac{1}{1-\nu}D_n(s)+E_n(s)\right]J_{n+1}(rs)\,ds = \begin{cases} g_1(r), & 0\le r<a,\\ g_2(r), & a<r<b,\\ g_3(r), & r>b,\end{cases} \quad (10)$$

where $f_1(r)$, $f_3(r)$, $g_1(r)$ and $g_3(r)$ are to be determined while $f_2(r)$ and $g_2(r)$ are given by $f_2(r)=1/2[a_n(r)-b_n(r)]$ and $g_2(r)=1/2[a_n(r)+b_n(r)]$, respectively, $n=1,2,3,\cdots$. Employing the Hankel inversion theorem, we obtain from (10)

$$\begin{aligned} D_n(s) &= \frac{1-\nu}{2}\sum_{i=1}^{3}\int_{\lambda_i}^{\lambda_{i+1}}\lambda[-f_i(\lambda)J_{n-1}(\lambda s) \\ &\quad +g_i(\lambda)J_{n+1}(\lambda s)]d\lambda, \\ E_n(s) &= \frac{1}{2}\sum_{i=1}^{3}\int_{\lambda_i}^{\lambda_{i+1}}\lambda[f_i(\lambda)J_{n-1}(\lambda s) \\ &\quad +g_i(\lambda)J_{n+1}(\lambda s)]d\lambda, \end{aligned} \quad (11)$$

where $\lambda_1=0$, $\lambda_2=a$, $\lambda_3=b$, $\lambda_4=\infty$. Substituting (11) into (8b), it is found that

$$\begin{aligned} &\sum_{i=1}^{3}\int_{\lambda_i}^{\lambda_{i+1}}\lambda[(2-\nu)f_i(\lambda)L_{n-1,n-1}(r,\lambda) \\ &\quad +\nu g_i(\lambda)L_{n-1,n+1}(r,\lambda)]d\lambda=0, \\ &\qquad 0\le r<a,\ r<b, \\ &\sum_{i=1}^{3}\int_{\lambda_i}^{\lambda_{i+1}}\lambda[\nu f_i(\lambda)L_{n+1,n-1}(r,\lambda) \\ &\quad +(2-\nu)g_i(\lambda)L_{n+1,n+1}(r,\lambda)]d\lambda=0, \\ &\qquad 0\le r<a,\ r>b, \end{aligned} \quad (12)$$

where $L_{n,m}(r,\lambda)$ is the Weber-Schafheitlin integral defined as $L_{n,m}(r,\lambda)=\int_0^\infty J_n(rs)J_m(\lambda s)\,ds$. With the help of the integral representation of the Weber-Schafheitlin integral $L_{n,m}(r,\lambda)$, it can be shown that (12) leads to the Abel's integral Eq. (B7), which appeared in Appendix B. S olving the Abel's integral Eq. (B7), we get the following mixed Volterra-Fredholm integral equations (See Appendix B for details):

$$\begin{aligned} &s^{2n-2}\Big[(\nu-2)F_1(s)+\nu G_1(s)+(\nu-2) \\ &\int_s^a \frac{1}{t}F_1(t)\,dt-\nu(2n-1)\int_s^a\frac{1}{t}G_1(t)\,dt\Big] \\ &+\int_b^\infty\{P_{13}(s,t)F_3(t)+P_{14}(s,t)G_3(t)\}dt \\ &=H_1(s), \qquad 0<s<a, \\ &s^{2n-2}[\nu F_1(s)+(\nu-2)G_1(s)]-\frac{2\nu n}{s} \\ &\int_0^s t^{2n-2}F_1(t)\,dt+\int_b^\infty\{P_{23}(s,t)F_3(t) \\ &+P_{24}(s,t)G_3(t)\}dt=H_2(s),\ 0<s<a, \\ &s^{-2n+2}[(\nu-2)F_3(s)+\nu G_3(s)]-2\nu ns \\ &\int_s^\infty\frac{G_3(t)}{t^{2n}}dt+\int_0^a\{P_{31}(s,t)F_1(t) \\ &+P_{32}(s,t)G_1(t)\}dt \\ &=H_3(s), \qquad b<s<\infty, \\ &s^{-2n+2}\Big[\nu F_3(s)+(\nu-2)G_3(s)-\frac{(2n+1)\nu}{s^2} \\ &\int_b^s tF_3(t)\,dt-\frac{\nu-2}{s^2}\int_b^s tG_3(t)\,dt\Big] \\ &+\int_0^a\{P_{41}(s,t)F_1(t)+P_{42}(s,t)G_1(t)\}dt \\ &=H_4(s), \qquad b<s<\infty, \end{aligned} \quad (13a)$$

where $F_i(s)$ and $G_i(s)$ $(i=1, 3)$ respectively are defined by

$$\begin{aligned} F_1(s) &= s^2\int_s^a\frac{f_1(\lambda)\,d\lambda}{\lambda^n\sqrt{\lambda^2-s^2}}, \\ G_1(s) &= s^2\int_s^a\frac{g_1(\lambda)\,d\lambda}{\lambda^n\sqrt{\lambda^2-s^2}}, \\ F_3(s) &= \int_b^s\frac{\lambda^n f_3(\lambda)\,d\lambda}{\sqrt{s^2-\lambda^2}}, \\ G_3(s) &= \int_b^s\frac{\lambda^n g_3(\lambda)\,d\lambda}{\sqrt{s^2-\lambda^2}}. \end{aligned} \quad (13b)$$

The kernels $P_{ij}(s,t)$ and $H_i(s)$ are presented in Appendix B. Regarding (13b) as the Abel's integral equation for $f_i(\lambda)$ and $g_i(\lambda)$ $(i=1, 3)$, $f_i(\lambda)$ and $g_i(\lambda)$ $(i=1, 3)$ are written in terms of $F_i(s)$ and $G_i(s)$ as

$$\begin{aligned} f_1(\lambda) &= -\frac{2}{\pi}\lambda^n\frac{d}{d\lambda}\int_\lambda^a\frac{F_1(s)\,ds}{\sqrt{s^2-\lambda^2}}, \\ g_1(\lambda) &= -\frac{2}{\pi}\lambda^n\frac{d}{d\lambda}\int_\lambda^a\frac{G_1(s)\,ds}{s\sqrt{s^2-\lambda^2}}, \\ f_3(\lambda) &= \frac{2}{\pi}\lambda^{-n}\frac{d}{d\lambda}\int_b^\lambda\frac{sF_3(s)\,ds}{\sqrt{\lambda^2-s^2}}, \end{aligned}$$

$$g_3(\lambda) = \frac{2}{\pi}\lambda^{-n}\frac{d}{d\lambda}\int_b^\lambda \frac{sG_3(s)\,ds}{\sqrt{\lambda^2 - s^2}}. \tag{14}$$

Once $F_1(s)$, $G_1(s)$, $F_3(s)$ and $G_3(s)$ are obtained from (13a), the displacements and stresses can be calculated.

4. Numerical Result and Discussion

4.1 Radial shear

Consider an annular crack subjected to radial shear $\tau_{zr} = a_0(r)$. In this case, (8a) and (8b) are reduced to the following equation:

$$\int_0^\infty sD_n(s)J_1(rs)\,ds = \frac{1-\nu}{2}a_0(r), \quad a < r < b, \tag{15}$$

$$\int_0^\infty D_n(s)J_1(rs)\,ds = 0, \quad 0 \le r < a, \quad r > b,$$
$$E_n(s) = 0. \tag{16}$$

The equation above is similar to that for the torsional problem investigated by Danyluk and Singh(1986). Following Danyluk and Singh (1986), it is obtained that

$$\tilde{F}_1(s) + \frac{2}{\pi}\int_b^\infty \left\{\frac{-s^2}{t(s^2-t^2)} + \frac{1}{2}\frac{s}{t^2}\log\frac{t+s}{t-s}\right\}\tilde{F}_3(t)\,dt = -\frac{1-\nu}{2}s^2\int_a^b \frac{a_0(t)\,dt}{\sqrt{t^2-s^2}}, \quad 0 < s < a,$$

$$\tilde{F}_3(s) + \frac{2}{\pi}\int_0^a \left\{\frac{s}{s^2-t^2} + \frac{1}{2t}\log\frac{s+t}{s-t}\right\}\tilde{F}_1(t)\,dt = -\frac{1-\nu}{2}\int_a^b \frac{t^2 a_0(t)}{\sqrt{s^2-t^2}}dt, \quad s > b, \tag{17a}$$

where

$$\tilde{F}_1(s) = s^2\int_s^a \frac{\tilde{f}_1(t)\,dt}{\sqrt{t^2-s^2}},$$

$$\tilde{F}_3(s) = \int_b^s \frac{t^2\tilde{f}_3(t)\,dt}{\sqrt{s^2-t^2}},$$

$$\int_0^\infty sD_n(s)J_1(rs)\,ds = \begin{cases}\tilde{f}_1(r), & 0 < r < a, \\ \tilde{f}_3(r), & r > b.\end{cases} \tag{17b}$$

The expression for the stress intensity factor at the inner edge and outer edge of the crack defined as

$$K_2^a = \lim_{r\to a^-}\sqrt{2\pi(a-r)}\,\tau_{zr}(r, \theta, 0),$$
$$K_2^b = \lim_{r\to b^+}\sqrt{2\pi(r-b)}\,\tau_{zr}(r, \theta, 0), \tag{18}$$

is reduced to

$$K_2^a = \frac{4}{1-\nu}\frac{\tilde{F}_1(a^-)}{a\sqrt{\pi a}},$$

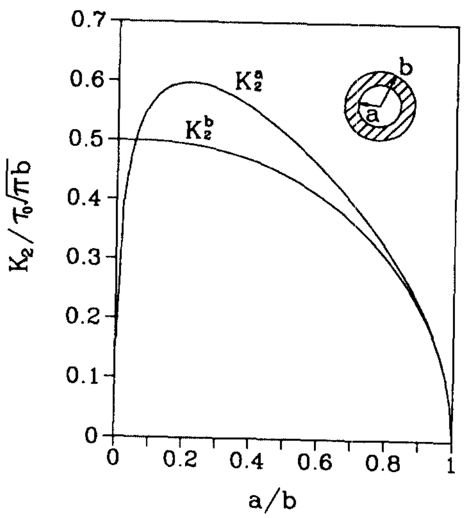

Fig. 2 Stress intensity factor K_2 at the inner (superscript a) and outer (superscript b) for annular crack under $\tau_{zr} = -\tau_0$

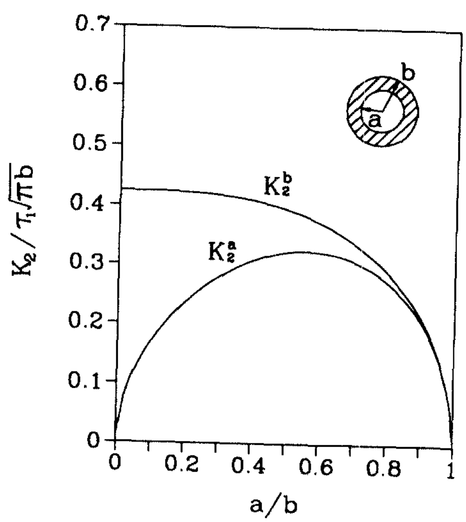

Fig. 3 Stress intensity factor K_2 at the inner (superscript a) and outer (superscript b) for annular crack under $\tau_{zr} = -\tau_1\frac{r}{b}$

$$K_2^b = \frac{4}{1-\nu}\frac{\tilde{F}_3(b^+)}{b\sqrt{\pi b}}. \qquad (19)$$

For the cases of $a_0(r) = -\tau_0$ (uniform radial shear) and $a_0(r) = -\tau_1\frac{r}{b}$ (linearly varying radial shear) respectively, numerical computation for the stress intensity factor are carried out. (The details will be described later.) In Fig. 2 and Fig. 3, the stress intensity factor K_2 at the inner edge (superscript a) and outer edge (superscript b) of the crack for the case of $a_0(r) = -\tau_0$ and $a_0(r) = -\tau_1\frac{r}{b}$, respectively, is plotted as a function of a/b. The numerical result for the case of $a_0(r) = -\tau_1\frac{r}{b}$ is in agreement with that for the torsional problem investigated by Choi and Shield(1982).

4.2 Shear load

Consider an annular crack subjected to a uniform shear $\tau_{zx} = -\tau_0$. In this case, $a_1 = -\tau_0$, $b_1 = \tau_0$ and a_n and b_n for $n \neq 1$ are all zero, since the boundary conditions are given by $q_c(r, \theta) = -\tau_0 \cos\theta$ and $q_s(r, \theta) = \tau_0 \sin\theta$. Substituting $n=1$, $f_2 = -\tau_0$ and $g_2 = 0$ into (13a), (13b), (B10) and (B11), we have the triple integral equation $(C1)$, which appeared in Appendix C where the kernels $P_{ij}(s, t)$ and $H_i(s)$ are given explicitly as a function of s and t (or s).

The stress intensity factor K_2 at the inner and outer edge of the crack is already defined by (18) and K_3 is given by the following form:

$$K_3^a = \lim_{r\to a^-}\sqrt{2\pi(a-r)}\,\tau_{z\theta}(r, \theta, 0),$$
$$K_3^b = \lim_{r\to b^+}\sqrt{2\pi(r-b)}\,\tau_{z\theta}(r, \theta, 0). \qquad (20)$$

It can be shown that $\tau_{zr}(r, \theta, 0)$ and $\tau_{z\theta}(r, \theta, 0)$ are given by

$$\tau_{zr}(r, \theta, 0) = \{g_i(r) + f_i(r)\}\cos\theta,$$
$$\tau_{z\theta}(r, \theta, 0) = \{g_i(r) - f_i(r)\}\sin\theta, \qquad (21)$$

where $i=1$ for $0 \le r < a$ and $i=3$ for $r > b$. Using integration by parts, it is found from (13b) with $n=1$, (18) (20) and (21) that

$$K_2^a = \cos\theta k_2^a, \qquad K_2^b = \cos\theta k_2^b,$$
$$K_3^a = -\sin\theta k_3^a, \qquad K_3^b = -\sin\theta k_3^b, \qquad (22)$$

where

$$k_2^a = \frac{2}{\sqrt{\pi a}}[G_1(a^-) + F_1(a^-)],$$
$$k_3^a = \frac{2}{\sqrt{\pi a}}[F_1(a^-) - G_1(a^-)],$$
$$k_2^b = \frac{2}{\sqrt{\pi b}}[G_3(b^+) + F_3(b^+)],$$
$$k_3^b = \frac{2}{\sqrt{\pi b}}[F_3(b^+) - G_3(b^+)]. \qquad (23)$$

In the limiting case as $a \to 0$, the integral Eq. $(C1)$ is reduced to a pair of Volterra equation, and the solution is given as (See Appendix D)

$$F_3(s) = \tau_0\left(s - \sqrt{s^2 - b^2}\right),$$
$$G_3(s) = \frac{\nu}{2-\nu}\frac{\tau_0 b^2}{s}. \qquad (24)$$

Using (22)~(24), it is obtained that

$$K_2^b = \frac{4\tau_0}{2-\nu}\sqrt{\frac{b}{\pi}}\cos\theta,$$
$$K_3^b = \frac{4\nu - 4}{2-\nu}\sqrt{\frac{b}{\pi}}\sin\theta, \qquad (25)$$

which correspond to the stress intensity factors for a penny-shaped crack with radius b under uniform shear (See Kassir and Sih, 1975).

A numerical solution of $(C1)$~$(C4)$, which appeared in Appendix C, may be obtained by

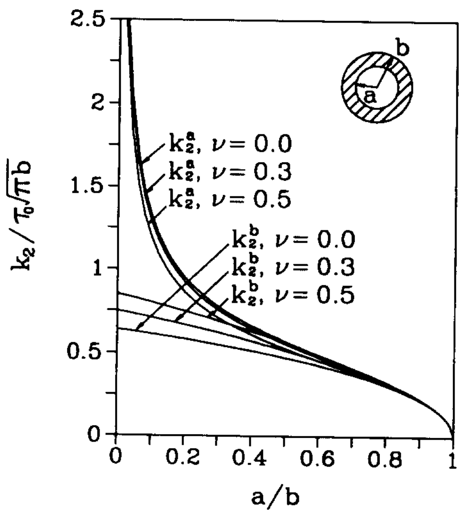

Fig. 4 Stress intensity factor k_2 at the inner (superscript a) and outer (superscript b) for annular crack under $\tau_{zx} = -\tau_0$

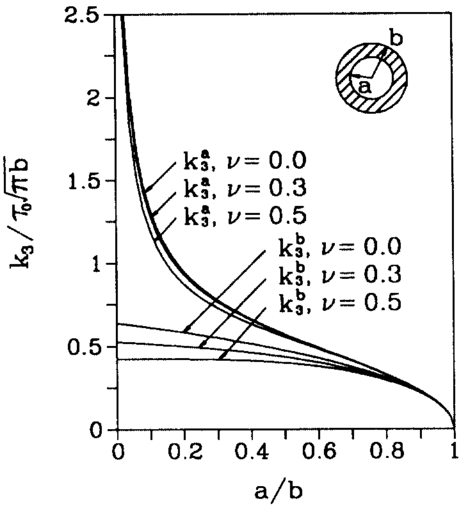

Fig. 5 Stress intensity factor k_3 at the inner (superscript a) and outer (superscript b) for annular crack under $\tau_{zx} = -\tau_0$

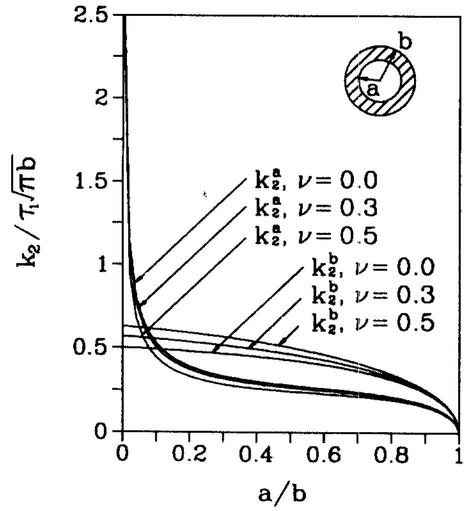

Fig. 6 Stress intensity factor k_2 at the inner (superscript a) and outer (superscript b) for annular crack under $\tau_{zx} = -\tau_1 \frac{r}{b}$

using some appropriate methods to evaluate the integral on the left hand side of ($C1$). Since the terms with varying integration range appear on the left hand sides of ($C1$), the integrals are approximately evaluated by means of the Simpson quadrature rule. For the convenience of the numerical calculation, we introduce new variable η defined by $s = a\eta$ for $F_1(s)$ and $G_1(s)$ and $s = b/\eta$ for $F_3(s)$ and $G_3(s)$. The mixed Volterra-Fredholm integral equation ($C1$) is reduced to the system of linear algebraic equations in $F_1(a\eta_k)$, $G_1(a\eta_k)$, $F_3(b/\eta_k)$ and $G_3(b/\eta_k)$ for selected values of η_k, which are solved numerically. In Fig. 4 and Fig. 5, the numerical results of the stress intensity factors k_2 at the inner and outer points (denoted by k_2^a and k_2^b respectively) and k_3 (denoted by k_3^a and k_3^b respectively) are shown as a function of a/b with various Poisson's ratio ν. In the limiting case as $a \to 0$, the result at the outer points is well compared with the case of the penny shaped crack, and k_2^a and k_3^a approach infinity. The values k_2 and k_3 for the small c at the point of the inner edge are greater than at the corresponding point of the outer edge.

Now we consider and annular crack subjected

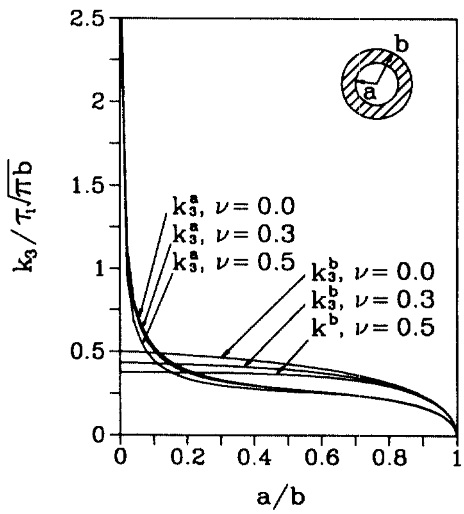

Fig. 7 Stress intensity factor k_3 at the inner (superscript a) and outer (superscript b) for annular crack under $\tau_{zx} = -\tau_1 \frac{r}{b}$

to shear traction (linearly varying shear) $\tau_{zx} = -\tau_1 \frac{r}{b}$. The solution procedure is similar to the case of uniform shear. The integral equation, the kernels $P_{ij}(s, t)$ and $H_i(s)$ for this problem are presented in Appendix C. In Fig. 6 and Fig. 7, the numerical result of the stress intensity factor is shown as a function of a/b with various Poisson's ratio ν. In the limiting case as $a \to 0$, the numerical result for k_2^b and k_3^b is in agreement with that for the penny-shaped crack (under linearly varying sherar) found in Kassir and Sih(1975).

5. Conclusion

An annular crack in an infinite isotropic elastic solid under shear loading is analyzed. In terms of mathematical difficulty, this work essentially requires determination of two harmonic functions in contrast to the determination of a single harmonic function in the previous works with the same geometry but under tensile or torsional loading. The solution method proposed here is amenable to easy numerical computation and the results under various shear loadings are presented. In particular, this work contains the result of some of the previous works as a limiting case.

References

Choi, I. and Shield, R. T., 1982, "A Note on a Flat Toroidal Crack in an Elastic Isotropic Body," Int. J.Solids Structures, Vol. 18, pp. 479～486.

Cooke, J. C., 1963, "Triple Integral Equations," Quart. J. Mech. Appl. Math., Vol. 16, pp. 193～203.

Danyluk, H. T. and Singh, B. M., 1986, Problem of an Infinite Solid Containing a Flat Annular Crack under Torsion," Engng Fracture Mech., Vol. 24, pp. 33～38.

Kassir, M. K. and Sih, G. C., 1975, "Three-Dimensional Crack Problems," In Mechanics of Fracture (Edited by G. C. Sih), Vol. 2, Noordhoff International Publishing, Leyden.

Kim, M. U. and Kim, J. U., 1985, "Slow Rotation of an annular Disk in a Viscous Fluid," J. Phys. Soc. Jpn., Vol. 54, pp. 3337～3341.

Moss, L. W. and Kobayashi, A. S., 1971, "Approximate Analysis of Axisymmetric Problems in Fracture Mechanics with Application to a Flat Toroidal Crack," Int. J. Fracture Mech., Vol. 7, pp. 89～99.

Panasyuk, V. V., Andrejkiv, A.E. and Stadnik. M. M., 1981, "Theree-Dimensional Static Crack Problems Solution (a Review)," Engng Fracture Mech., Vol. 14, pp. 245～260.

Selvadurai, A. P. S. and Singh, B. M., 1985, "The Annular Crack Problem for an Isotropic Elastic Solid," Quart. J. Mech. Appl. Math., Vol. 38, pp. 233～243.

Smetanin, B. I., 1968, "Problem of Extension of an Elastic Space Containing a plane Annular Slit," PMM, J. Appl. Math. Mech., Vol. 32, pp. 458～462.

Sneddon, I. N., 1946, "The Distribution of stress in the Neighborhood of acrack in an Elastic Solid," Proc. Roy. Soc. (London) A, Vol. 187, pp. 229～260.

Watson, G. N., 1944, "Theory of Bessel Functions," Cambridge University Press, London.

Appendix A. General Solution of the Navier's Equilibrium Equation

We employ the method described in Kim and Kim(1985) for the Stokes flow to obtain a general solution of the Navier's equilibrium equation in terms of three harmonic functions. Introducing the Cartesian coordinate, (1) is written as

$$u_{i,jj} + \frac{1}{1-2\nu} e_{,i} = 0, \tag{A1}$$

$$e = u_{j,j}, \tag{A2}$$

where the comma(,) denotes the partial derivative with respect to the Cartesian coordinate and subscripts i, $j = 1, 2, 3$. Noting that the dilatation e is harmonic, we may write e in the form

$$2\mu e = -(2-4\nu)\,\phi_{,3}, \tag{A3}$$

where ϕ is a harmonic function. From (A1) with $i=3$ and (A3), we get

$$2\mu u_{3,jj} = 2\phi_{,33}. \tag{A4}$$

We may write a general solution of (A4) in the form

$$2\mu u_3 = x_3\phi_{,3} - \alpha\phi + \chi_{,3}, \tag{A5}$$

where χ is a harmonic function. Put

$$2\mu u_1 = x_3\phi_{,1} + \chi_{,1} + \Psi_1, \tag{A6}$$

$$2\mu u_2 = x_3\phi_{,2} + \chi_{,2} + \Psi_2. \tag{A7}$$

We determine α and the general forms of Ψ_1 and Ψ_2 so as to satisfy (A1) and (A2). Substituting (A3) and (A5)~(A7) into (A2), we have

$$\Psi_1 = \Psi_{,2}, \quad \Psi_2 = -\Psi_{,1}, \tag{A8}$$

and $\alpha = 3\text{-}4\nu$. Substituting (A3), (A6) and (A7) together with (A8) into (A1) for $i=1$, 2 yields

$$\Psi_{,jj2} = -\Psi_{,jj1} = 0, \tag{A9}$$

The equation above shows that $\Psi_{,jj}$ is a function of x_3 only, which may be taken as 0 since only $\Psi_{,1}$ and $\Psi_{,2}$ contribute to u_1 and u_2. Consequently Ψ is a harmonic function. In summary, a general solution of the Navier's equilibrium equation is expressed as

$$2\mu u_1 = x_3\phi_{,1} + \chi_{,1} + \Psi_{,2},$$
$$2\mu u_2 = x_3\phi_{,2} + \chi_{,2} - \Psi_{,1},$$
$$2\mu u_3 = x_3\phi_{,3} - (3\text{-}4\nu)\phi + \chi_{,3}, \tag{A10}$$

where ϕ, χ and Ψ are harmonic functions. For the cylindrical coordinate, (A10) is rewritten as (2).

Appendix B. Solution of a Pair of Triple Integral Equations

A method of solution for a pair of the triple integral Eqs. (8a) and (8b) involving the Bessel functions is presented. A pair of the integral Eqs. (8a) and (8b) lead to the mixed Volterra-Fredholm integral equations. Using the second equation in (9), the Weber-Schafheitlin ingegral $L_{n+1,n-1}(r, \lambda)$ is written as

$$L_{n+1,n-1}(r, \lambda) = \frac{2n}{\lambda}M_{n+1,n}(r, \lambda) - L_{n+1,n+1}(r, \lambda),$$
$$= \frac{2n}{r}M_{n,n-1}(r, \lambda) - L_{n-1,n-1}(r, \lambda), \tag{B1}$$

where

$$M_{n,m} = \int_0^\infty \frac{1}{s}J_n(rs)\, J_m(\lambda s)ds.$$

$M_{n,n-1}(r, \lambda)$ is expressed in terms of the hypergeometric function (Watson, 1944) as

$$M_{n,n-1}(r, \lambda) = \begin{cases} \dfrac{\lambda^{n-1}\Gamma(n-1/2)}{2r^{n-1}\Gamma(3/2)\Gamma(n)}F(n-1/2,\ -1/2,\ n;\lambda^2/r^2), & 0<\lambda<r, \\ \dfrac{r^n\Gamma(n-1/2)}{2\lambda^n\Gamma(n+1)}F(n-1/2,\ 1/2,\ n+1;r^2/\lambda^2), & 0<r<\lambda. \end{cases} \tag{B2}$$

where $n=1, 2, 3, \cdots$, $\Gamma(x)$ is the gamma function and $F(a, b, c; z)$ is the hypergeometric function defined as

$$F(a, b, c; z) = \frac{\Gamma(c)}{\Gamma(a)\Gamma(c-a)} \int_0^1 t^{a-1}(1-t)^{c-a-1}(1-tz)^{-b}dt. \tag{B3}$$

Using (B1)~(B3) and the expression of $L_{n,n}(r, \lambda)$ presented in Cooke(1963), the Weber-Schafheitlin integral is written in the form:

$$L_{n,n}(r, \lambda) = \frac{2}{\pi}r^{-n}\lambda^{-n}\int_0^{min(r,\lambda)} \frac{s^{2n}ds}{\sqrt{r^2-s^2}\sqrt{\lambda^2-s^2}} = \frac{2}{\pi}r^n\lambda^n\int_{max(r,\lambda)}^\infty \frac{ds}{s^{2n}\sqrt{s^2-r^2}\sqrt{s^2-\lambda^2}},$$

$$L_{n-1,n+1}(r, \lambda) = \frac{2}{\pi}r^{-n+1}\lambda^{-n-1}\int_0^{min(r,\lambda)} \frac{(2n-1)\lambda^2 - 2ns^2}{\sqrt{r^2-s^2}\sqrt{\lambda^2-s^2}}s^{2n-2}ds = \frac{2}{\pi}r^{n-1}\lambda^{n-1}\int_{max(r,\lambda)}^\infty \frac{(2n-1)s^2-2nr^2}{\sqrt{s^2-r^2}\sqrt{s^2-\lambda^2}}\frac{ds}{s^{2n}},$$

$$L_{n+1,n-1}(r, \lambda) = \frac{2}{\pi}r^{-n-1}\lambda^{-n-1}\int_0^{min(r,\lambda)} \frac{2nr^2-(2n+1)s^2}{\sqrt{r^2-s^2}\sqrt{\lambda^2-s^2}}s^{2n}ds = \frac{2}{\pi}r^{n+1}\lambda^{n-1}\int_{max(r,\lambda)}^\infty \frac{2ns^2-(2n+1)\lambda^2}{\sqrt{s^2-r^2}\sqrt{s^2-\lambda^2}}\frac{ds}{s^{2n+2}}. \tag{B4}$$

For the functions $G_i(s)$ and $G(s)$ $(i=1,\ 3)$ defined in (13b), it can be shown that

$$\int_s^a \frac{f_1(\lambda)\,d\lambda}{\lambda^{n-2}\sqrt{\lambda^2-s^2}} = F_1(s) + \int_s^a \frac{F_1(t)}{t}dt,$$

$$\int_s^a \frac{g_1(\lambda)\,d\lambda}{\lambda^{n-2}\sqrt{\lambda^2-s^2}} = G_1(s) + \int_s^a \frac{G_1(t)}{t}dt,$$
$$\int_b^s \frac{\lambda^{n+2} f_3(\lambda)}{\sqrt{s^2-\lambda^2}}d\lambda = s^2F_3(s) - \int_b^s tF_3(t)\,dt,$$
$$\int_b^s \frac{\lambda^{n+2} g_3(\lambda)}{\sqrt{s^2-\lambda^2}}d\lambda = s^2G_3(s) - \int_b^s tG_3(t)\,dt,$$
$$r^2\int_0^r \frac{s^{2n-2}F_1(s)}{\sqrt{r^2-s^2}}ds = \int_0^r\Big[s^{2n}F_1(s) + s\int_0^s t^{2n-2}F_1(t)\,dt\Big]\frac{ds}{\sqrt{r^2-s^2}},$$
$$r^2\int_r^\infty \frac{F_3(s)\,ds}{s^{2n}\sqrt{s^2-r^2}} = \int_r^\infty\Big[\frac{F_3(s)}{s^{2n-2}} - s\int_s^\infty \frac{F_3(t)}{t^{2n}}dt\Big]\frac{ds}{\sqrt{s^2-r^2}}. \quad \text{(B5)}$$

Using (B4), (B5) and the relations

$$\int_0^a d\lambda\int_0^{min(r,\lambda)} ds = \int_0^r ds\int_s^a d\lambda,\ 0\le r<a,$$
$$\int_a^b d\lambda\int_0^{min(r,\lambda)} ds = \int_0^r ds\int_a^s d\lambda,\ 0\le r<a,$$
$$\int_b^\infty d\lambda\int_{max(r,\lambda)}^\infty ds = \int_b^\infty ds\int_b^s d\lambda,\ 0\le r<a,$$
$$\int_0^a d\lambda\int_0^{min(r,\lambda)} ds = \int_0^a ds\int_s^a d\lambda,\ r>b,$$
$$\int_a^b d\lambda\int_{max(r,\lambda)}^\infty ds = \int_r^\infty ds\int_a^b d\lambda,\ r>b,$$
$$\int_b^\infty d\lambda\int_{max(r,\lambda)}^\infty ds = \int_r^\infty ds\int_b^\infty d\lambda,\ r>b, \quad \text{(B6)}$$

we obtain from (12) the following Abel's integral equations:

$$\int_0^r s^{2n-2}\Big[(\nu-2)F_1(s) + \nu G_1(s) + (\nu-2)\int_s^a t^{-1}F_1(t)\,dt - \nu(2n-1)\int_s^a t^{-1}G_1(t)\,dt + \int_a^b\{(\nu-2)\lambda^2 f_2(\lambda) - \nu((2n-1)\lambda^2 - 2ns^2)g_2(\lambda)\}\frac{d\lambda}{\lambda^n\sqrt{\lambda^2-s^2}}\Big]\frac{ds}{\sqrt{r^2-s^2}}$$
$$= -r^{2n-2}\int_b^\infty[(\nu-2)t^2F_3(t) - \nu(2n-1)t^2G_3(t) + 2\nu nr^2G_3(t)]\frac{dt}{t^{2n}\sqrt{t^2-r^2}}, \quad 0\le r<a,$$

$$\int_0^r\Big[s^{2n}\{\nu F_1(s) + (\nu-2)G_1(s)\} - 2\nu ns\int_0^s t^{2n-2}F_1(t)\,dt + s^{2n+2}\int_a^b\{\nu f_2(\lambda) + (\nu-2)g_2(\lambda)\}\frac{d\lambda}{\lambda^n\sqrt{\lambda^2-s^2}} - 2\nu ns\int_0^s t^{2n}\Big\{\int_a^b\frac{f_2(\lambda)\,d\lambda}{\lambda^n\sqrt{\lambda^2-t^2}}\Big\}dt\Big]\frac{ds}{\sqrt{r^2-s^2}} = -r^{2n+2}\int_b^\infty$$
$$\Big[\nu\frac{F_3(t)}{t^{2n}} - \frac{2n+1}{t^{2n+2}}\nu\int_b^t uF_3(u)\,du + (\nu-2)\frac{G_3(t)}{t^{2n}} - \frac{\nu-2}{t^{2n+2}}\int_b^t uG_3(u)\,du\Big]\frac{dt}{\sqrt{t^2-r^2}}, \quad 0\le r<a,$$

$$\int_r^\infty\Big[s^{-2n+2}\{(\nu-2)F_3(s) + \nu G_3(s)\} - 2\nu ns\int_s^\infty t^{-2n}G_3(t)\,dt + s^{-2n+2}\int_a^b\{(\nu-2)f_2(\lambda) + \nu g_2(\lambda)\}\frac{\lambda^n d\lambda}{\sqrt{s^2-\lambda^2}} - 2\nu ns\int_s^\infty t^{-2n}\Big\{\int_a^b\frac{\lambda^n g_2(\lambda)\,d\lambda}{\sqrt{s^2-\lambda^2}}\Big\}dt\Big]\frac{ds}{\sqrt{s^2-r^2}} = -r^{-2n+2}\int_0^a$$
$$\Big[(\nu-2)F_1(t) + \nu G_1(t) + (\nu-2)\int_t^a u^{-1}F_1(u)\,du - (2n-1)\nu\int_t^a u^{-1}G_1(u)\,du\Big]\frac{t^{2n-2}dt}{\sqrt{r^2-t^2}}, \quad r>b,$$

$$\int_r^\infty s^{-2n-2}\Big[\nu s^2F_3(s) + (\nu-2)s^2G_3(s) - (2n+1)\nu\int_b^s tF_3(t)\,dt - (\nu-2)\int_b^s tG_3(t)\,dt + \int_a^b\{-2\nu ns^2\lambda^n f_2(\lambda) + (2n+1)\nu\lambda^{n+2}f_2(\lambda) + (\nu-2)\lambda^{n+2}g_2(\lambda)\}\frac{d\lambda}{\sqrt{s^2-\lambda^2}}\Big]\frac{ds}{\sqrt{s^2-r^2}} = -r^{-2n-2}\int_0^a$$
$$[-2\nu nr^2t^{2n-2}F(t) + (2n+1)\nu t^{2n}F_1(t) + (\nu-2)t^{2n}G_1(t)]\frac{dt}{\sqrt{r^2-t^2}}, \quad r>b. \quad \text{(B7)}$$

Solving the Abel's integral Eq. (B7) with the relation

$$\int_b^\infty t^{-2n-2}V_{n+1}(s,t)\Big\{\int_b^t uF_3(u)\,du\Big\}dt = \int_b^\infty \tilde{V}_{n+1}(s,t)\,tF_3(t)\,dt,$$
$$\int_0^a t^{2n-2}U_{n-1}(s,t)\Big\{\int_t^a u^{-1}F_1(u)\,du\Big\}dt = \int_0^a \tilde{U}_{n-1}(s,t)\,t^{-1}F_1(t)\,dt, \quad \text{(B8)}$$

where

$$U_n(s,t)=\frac{d}{ds}\int_s^\infty \frac{r^{-2n+1}dr}{\sqrt{r^2-s^2}\sqrt{r^2-t^2}},$$
$$V_n(s,t)=\frac{d}{ds}\int_0^s \frac{r^{2n+1}dr}{\sqrt{s^2-r^2}\sqrt{t^2-r^2}},$$
$$\tilde{U}_n(s,t)=\int_0^t u^{2n}U_n(s,u)\,du,$$
$$\tilde{V}_n(s,t)=\int_t^\infty u^{-2n}V_n(s,u)\,du, \qquad \text{(B9)}$$

we finally obtain (13a), Here the kernels $P_{ij}(s,t)$ are given as

$$P_{13}(s,t)=\frac{2}{\pi}(\nu-2)\,t^{-2n+2}\frac{d}{ds}\int_0^s \frac{\xi^{2n-1}d\xi}{\sqrt{s^2-\xi^2}\sqrt{t^2-\xi^2}},$$
$$P_{14}(s,t)=\frac{2\nu}{\pi}\frac{d}{ds}\Big[-\frac{2n-1}{t^{2n-2}}\int_0^s \frac{\xi^{2n-1}d\xi}{\sqrt{s^2-\xi^2}\sqrt{t^2-\xi^2}}+\frac{2n}{t^{2n}}\int_0^s \frac{\xi^{2n+1}d\xi}{\sqrt{s^2-\xi^2}\sqrt{t^2-\xi^2}}\Big],$$
$$P_{23}(s,t)=\frac{2\nu}{\pi}\Big[\frac{1}{s^2t^{2n}}\frac{d}{ds}\int_0^s \frac{\xi^{2n+3}d\xi}{\sqrt{s^2-\xi^2}\sqrt{t^2-\xi^2}}-\frac{(2n+1)t}{s^2}\frac{d}{ds}\int_t^\infty\int_0^s \frac{\xi^{2n+3}u^{-2n-2}d\xi du}{\sqrt{s^2-\xi^2}\sqrt{u^2-\xi^2}}\Big],$$
$$P_{24}(s,t)=\frac{2}{\pi}(\nu-2)\Big[\frac{1}{s^2t^{2n}}\frac{d}{ds}\int_0^s \frac{\xi^{2n+3}d\xi}{\sqrt{s^2-\xi^2}\sqrt{t^2-\xi^2}}-\frac{t}{s^2}\frac{d}{ds}\int_t^\infty\int_0^s \frac{\xi^{2n+3}u^{-2n-2}d\xi du}{\sqrt{s^2-\xi^2}\sqrt{u^2-\xi^2}}\Big],$$
$$P_{31}(s,t)=\frac{2}{\pi}(2-\nu)\Big[t^{2n-2}\frac{d}{ds}\int_s^\infty \frac{\xi^{-2n+3}d\xi}{\sqrt{\xi^2-s^2}\sqrt{\xi^2-t^2}}+\frac{1}{t}\frac{d}{ds}\int_0^t\int_s^\infty \frac{\xi^{-2n+3}u^{2n-2}d\xi du}{\sqrt{\xi^2-s^2}\sqrt{\xi^2-u^2}}\Big],$$
$$P_{32}(s,t)=\frac{2}{\pi}\nu\Big[-t^{2n-2}\frac{d}{ds}\int_s^\infty \frac{\xi^{-2n+3}d\xi}{\sqrt{\xi^2-s^2}\sqrt{\xi^2-t^2}}+\frac{2n-1}{t}\frac{d}{ds}\int_0^t\int_s^\infty \frac{\xi^{-2n+3}u^{2n-2}d\xi du}{\sqrt{\xi^2-s^2}\sqrt{\xi^2-u^2}}\Big],$$
$$P_{41}(s,t)=\frac{2}{\pi}\nu s^2t^{2n-2}\frac{d}{ds}\int_s^\infty \frac{[2n\xi^{-2n+1}-(2n+1)t^2\xi s^{-2n-1}]}{\sqrt{\xi^2-s^2}\sqrt{\xi^2-t^2}}d\xi,$$
$$P_{42}(s,t)=\frac{2}{\pi}(2-\nu)s^2t^{2n}\frac{d}{ds}\int_s^\infty \frac{\xi^{-2n-1}d\xi}{\sqrt{\xi^2-s^2}\sqrt{\xi^2-t^2}}, \qquad \text{(B10)}$$

and the functions $H_i(s)$ $(i=1,\cdots,4)$ are given as

$$H_1(s)=s^{2n-2}\int_a^b[(2-\nu)\xi^2f_2(\xi)+\nu\{(2n-1)\xi^2-2ns^2\}g_2(\xi)]\frac{d\xi}{\xi^n\sqrt{\xi^2-s^2}},$$
$$H_2(s)=s^{2n}\int_a^b[-\nu f_2(\xi)-(\nu-2)g_2(\xi)]\frac{d\xi}{\xi^n\sqrt{\xi^2-s^2}}+\frac{2\nu n}{s}\int_o^s t^{2n}\int_a^b\frac{f_2(\xi)\,d\xi}{\xi^n\sqrt{\xi^2-t^2}}dt,$$
$$H_3(s)=s^{-2n+2}\int_a^b\{\frac{2-\nu)\xi^nf_2(\xi)-\nu\xi^ng_2(\xi)\}}{\sqrt{s^2-\xi^2}}d\xi+2\nu ns\int_s^\infty t^{-2n}\int_a^b\frac{\xi^ng_2(\xi)\,d\xi}{\sqrt{t^2-\xi^2}}dt,$$
$$H_4(s)=s^{-2n}\int_a^b[\{2\nu ns^2\xi^n-(2n+1)\nu\xi^{n+2}\}f_2(\xi)-(\nu-2)\xi^{n+2}g_2(\xi)\}\frac{d\xi}{\sqrt{s^2-\xi^2}}. \qquad \text{(B11)}$$

Appendix C. Shear Load

The integral equations for the problem of the annular crack under shear traction $\tau_{zx}=-\tau(r)$ are written as

$$(\nu-2)F_1(s)+\nu G_1(s)+(\nu-2)\int_s^a\frac{1}{t}F_1(t)\,dt-\nu\int_s^a\frac{1}{t}G_1(t)\,dt+\int_b^\infty\{P_{13}(s,t)F_3(t)+P_{14}(s,t)G_3(t)\}dt=H_1(s), \qquad 0<s<a,$$
$$\nu F_1(s)+(\nu-2)G_1(s)]-\frac{2\nu}{s}\int_0^s F_1(t)\,dt+\int_b^\infty\{P_{23}(s,t)F_3(t)+P_{24}(s,t)G_3(t)\}dt=H_2(s), \qquad 0<s<a,$$
$$(\nu-2)F_3(s)+\nu G_3(s)-2\nu s\int_s^\infty\frac{G_3(t)}{t^2}dt+\int_0^a\{P_{31}(s,t)F_1(t)+P_{32}(s,t)G_1(t)\}dt=H_3(s), \qquad s>b,$$

$$\nu F_3(s)+(\nu-2)G_3(s)-\frac{3\nu}{s^2}\int_b^s tF_3(t)\,dt-\frac{\nu-2}{s^2}\int_b^s tG_3(t)\,dt+\int_0^a\{P_{41}(s,t)F_1(t)+P_{42}(s,t)G_1(t)\}dt=H_4(s),\qquad s>b. \qquad \text{(C1)}$$

Here $F_i(s)$ and $G_i(s)$ $(i=1, 3)$ are defined as

$$F_1(s)=s^2\int_s^a\frac{f_1(\lambda)\,d\lambda}{\lambda\sqrt{\lambda^2-s^2}},$$
$$G_1(s)=s^2\int_s^a\frac{g_1(\lambda)\,d\lambda}{\lambda\sqrt{\lambda^2-s^2}},$$
$$F_3(s)=\int_b^s\frac{\lambda f_3(\lambda)\,d\lambda}{\sqrt{s^2-\lambda^2}},$$
$$G_3(s)=\int_b^s\frac{\lambda g_3(\lambda)\,d\lambda}{\sqrt{s^2-\lambda^2}}. \qquad \text{(C2)}$$

The kernels $P_{ij}(s, t)$ are given as

$$P_{13}(s,t)=\frac{2}{\pi}(\nu-2)\frac{t}{t^2-s^2},$$
$$P_{14}(s,t)=\frac{2}{\pi}\nu\left[\frac{2s^2-t^2}{t(t^2-s^2)}+\frac{s}{t^2}\log\frac{t+s}{t-s}\right],$$
$$P_{23}(s,t)=\frac{2}{\pi}\nu\left[\frac{t}{t^2-s^2}-\frac{1}{2s}\log\frac{t+s}{t-s}\right],$$
$$P_{24}(s,t)=\frac{2}{\pi}(\nu-2)\left[\frac{s^2}{t(t^2-s^2)}+\frac{s}{2t^2}\log\frac{t+s}{t-s}\right],$$
$$P_{31}(s,t)=\frac{2}{\pi}(\nu-2)\left[\frac{s}{s^2-t^2}+\frac{1}{2t}\log\frac{s+t}{s-t}\right],$$
$$P_{32}(s,t)=\frac{2}{\pi}\nu\left[\frac{s}{s^2-t^2}-\frac{1}{2t}\log\frac{s+t}{s-t}\right],$$
$$P_{41}(s,t)=\frac{2}{\pi}\nu\left[\frac{9t^2-7s^2}{2s(s^2-t^2)}+\frac{9t^2-s^2}{4ts^2}\log\frac{s+t}{s-t}\right],$$
$$P_{42}(s,t)=\frac{2}{\pi}(\nu-2)\left[\frac{3t^2-s^2}{2s(s^2-t^2)}+\frac{3t^2+s^2}{4ts^2}\log\frac{s+t}{s-t}\right]. \qquad \text{(C3)}$$

The functions $H_i(s)$ for the case of $\tau_{zx}=-\tau_0$ are given in the form:

$$H_1(s)=(\nu-2)\tau_0\left[\sqrt{b^2-s^2}-\sqrt{a^2-s^2}\right],$$
$$H_2(s)=\nu\tau_0\left[\frac{b^2}{2s}\cos^{-1}\frac{s}{b}-\frac{a^2}{2s}\cos^{-1}\frac{s}{a}+\frac{1}{2}\sqrt{b^2-s^2}-\frac{1}{2}\sqrt{a^2-s^2}-\frac{\pi}{4}\frac{b^2}{s}+\frac{\pi}{4}\frac{a^2}{s}\right],$$
$$H_3(s)=(\nu-2)\tau_0\left[\sqrt{s^2-a^2}-\sqrt{s^2-b^2}\right],$$
$$H_4(s)=\nu\tau_0\left[\frac{a^2}{s^2}\sqrt{s^2-a^2}-\frac{b^2}{s^2}\sqrt{s^2-b^2}\right]. \qquad \text{(C4)}$$

The functions $H_i(s)$ for the case of $\tau_{zx}=-\tau_1\frac{r}{b}$ are given in the form:

$$H_1(s)=\frac{\tau_1}{2b}(\nu-2)\left[b\sqrt{b^2-s^2}-a\sqrt{a^2-s^2}+s^2\log\left\{+\left(b\sqrt{b^2-s^2}\right)\Big/\left(a+\sqrt{a^2-s^2}\right)\right\}\right],$$
$$H_2(s)=\frac{\nu\tau_1}{3b}\left[b\sqrt{b^2-s^2}-a\sqrt{a^2-s^2}+s^2\log\left\{\left(b+\sqrt{b^2-s^2}\right)\Big/\left(a+\sqrt{a^2-s^2}\right)\right\}-\frac{b^3}{s}\sin^{-1}\frac{s}{b}+\frac{a^3}{s}\sin^{-1}\frac{s}{a}\right],$$
$$H_3(s)=\frac{\tau_1}{2b}(\nu-2)\left[a\sqrt{s^2-a^2}-b\sqrt{s^2-b^2}+s^2\sin^{-1}\frac{b}{s}-s^2\sin^{-1}\frac{a}{s}\right],$$
$$H_4(s)=\frac{\nu\tau_1}{b}\left[-\left(\frac{3}{4}\frac{b^3}{s^2}+\frac{1}{8}b\right)\sqrt{s^2-b^2}+\left(\frac{3}{4}\frac{a^3}{s^2}+\frac{1}{8}a\right)\sqrt{s^2-a^2}+\frac{1}{8}s^2\left(\sin^{-1}\frac{b}{s}-\sin^{-1}\frac{a}{s}\right)\right]. \qquad \text{(C5)}$$

Appendix D. Solution of Uniform Shear for the Case of $a\to 0$

In the limiting case as $a\to 0$, (C1) is reduced to the following Volterra equation:

$$(\nu-2)F_3(s)+\nu G_3(s)-2\nu s\int_s^\infty\frac{G_3(t)}{t^2}dt=H_3(s),$$

$$\nu F_3(s)+(\nu-2)G_3(s)-\frac{3\nu}{s^2}\int_b^s tF_3(t)\,dt$$
$$-\frac{\nu-2}{s^2}\int_b^s tG_3(t)\,dt=H_4(s), \qquad \text{(D1)}$$

where

$$H_3(s)=(\nu-2)\tau_0\left[s-\sqrt{s^2-b^2}\right],$$
$$H_4(s)=-\nu\tau_0\frac{b^2}{s^2}\sqrt{s^2-b^2}. \qquad \text{(D2)}$$

From (D1) and (D2), it is obtained that

$$sF_3'(s)-F_3(s)=-\frac{\tau_0 b^2}{\sqrt{s^2-b^2}},$$
$$sG_3'(s)+G_3(s)=0. \qquad \text{(D3)}$$

Solving (D3), we get

$$F_3(s)=\alpha s-\tau_0\sqrt{s^2-b^2},$$
$$G_3(s)=\frac{\beta}{s}. \qquad \text{(D4)}$$

where α and b are constant. Using (D4) and (D1) with $s=b$, it can be shown that

$$\alpha=\tau_0,$$
$$\beta=\frac{\nu}{2-\nu}\tau_0 b^2. \qquad \text{(D5)}$$

Form (D4) and (D5), (25) is obtained.